

Effect of Carbide Size and Distribution on Weldability of Low-Carbon Steels

Martensite networks can be formed in 0.08%C steel when carbides dissolve heterogeneously in austenite during rapid thermal cycles, such as those which occur in resistance welding

BY W. F. SAVAGE, E. F. NIPPES AND R. J. HAGLER

ABSTRACT. When seam welded tubing is made from different heats of plain, low-C steel having similar chemical compositions, tubing from a particular heat will often fail in a brittle manner. The only apparent difference in the original microstructures of these steels is the size and distribution of iron carbides.

Because these steels have less than 0.10%C and brittle martensite generally is associated with a C content in excess of 0.20%, a study of non-equilibrium phase changes which occur in welding was undertaken.

A C gradient occurs when an iron carbide particle of 6.67%C is dissolving in austenite. When this C gradient exists and the material is cooled rapidly, areas of high-C martensite may form. The diffusion distance of C is mainly dependent on the temperature and time; therefore, the diffusion distance will be constant for a particular thermal cycle. As the carbide size becomes smaller, the distance between particles decreases. If this distance is smaller than twice the diffusion distance and the steel is cooled rapidly, a continuous network of martensite will exist.

The Gleeble was used to subject specimens to various thermal cycles and peak temperatures. Microhardness and Vickers hardness readings revealed the presence of hard areas, and metallographic examination indicated that these areas consisted of high-C martensite. Thus, as a consequence of the lack of homogeneity in the austenite produced by rapid thermal cycles, brittle martensite networks were formed. The extent of these networks was dependent on the size and distribution of the carbides.

Good correlation was found be-

tween the observed and calculated diffusion distances, when these values were plotted as a function of the reciprocal of the absolute temperature.

Introduction

A considerable proportion of the tubing made for pressure application is electric-resistance seam welded using low-carbon steel. A major problem in the manufacture of such tubing is the different welding characteristics of various heats. These have essentially identical compositions but differ markedly in their ability to pass standard inspection tests without failing in a brittle manner. Upon metallographic examination in the as-received condition, the only apparent difference in these heats is the size and distribution of iron-carbide particles.

As early as 1939, Babcock¹ discussed the microstructural changes taking place during welding thermal cycles in a 0.25%C steel and illustrated, with the use of the Fe-Fe₃C equilibrium diagram, the effects of non-equilibrium heating and cooling. A similar effect of non-equilibrium conditions was described by Stout and Doty² for a 0.25%C steel which was oil quenched after heating into the transformation range. This steel exhibited a microstructure of ferrite, pearlite, and high-carbon martensite. Recently, Gould³ showed that the major factor which

influenced the induction hardening of SAE 4150 steel was the size of the iron carbides. In this instance, fine carbides gave a harder and more uniform case; therefore, a control on the carbide size was used to insure a reliable, heat-treated product.

A detailed study of the formation of austenite at high heating rates was made by Huggins, *et al.*⁴ However, in his investigation, the dissolution of iron carbides was studied for medium and high C steels.

In the cases discussed above, no investigation was performed on steels having a C content less than 0.10%. Furthermore, no investigation has been reported which cited the presence of a martensitic network in plain-carbon steels of such a low C content.

When steels that have been subjected to a welding thermal cycle fail in a brittle manner, the cause can often be attributed to the presence of martensite. Generally, martensite is excessively brittle only when the C content of the austenite from which it transforms exceeds approximately 0.20%. However, the possibility exists that a network of brittle martensite can be formed in resistance welds in a plain carbon steel of less than 0.10%C, when the size and distribution of the carbides is unfavorable.

Under equilibrium conditions, plain C steels with a C content of 0.08% exist at room temperature as ferrite and cementite. Although the Fe-Fe₃C diagram indicates the phases present in steels only for equilibrium conditions, this diagram can also be used to explain certain non-equilibrium conditions experienced in welding. When a 0.08%C steel is heated to the A₃ temperature, approximately 1635 F

W. F. SAVAGE is Professor of Metallurgical Engineering and Director of Welding Research, and E. F. NIPPES is Professor of Metallurgical Engineering, Rensselaer Polytechnic Institute, Troy, New York. R. J. HAGLER, former G.M.I. Graduate Fellow at RPI, is with Lovejoy Inc., Downer's Grove, Illinois.

(890 C), the diagram indicates that only austenite will be present if sufficient time is allowed for equilibrium to be established. When a 0.08%C steel is heated rapidly to a temperature of 1530 F (832 C), the phases that can exist at this temperature are ferrite (with a maximum %C of approximately 0.01%), austenite (with a composition approximately from 0.19 to 1.02%), and iron carbide (with 6.67% C).

Assuming the iron-carbide particle has not dissolved completely, a schematic representation can be made of the C gradient around the carbide, as shown in Fig. 1. When this condition exists and the alloy is subjected to rapid cooling, the volume of material which had transformed to austenite on heating may transform to martensite if the cooling rate exceeds the critical cooling rate for the austenite formed. The amount of austenite formed in the intercritical region depends upon the diffusion distance, $4(Dt)^{1/2}$, i.e., four times the square root of Dt , where D is the diffusivity of C at the particular temperature and t is the effective time at that temperature.⁵

Almost all of the C present in a low-carbon steel is initially in the form of iron carbide. If the carbides are assumed to be spherical with a completely random distribution, the mean distance between carbides is approximately 5 times the radius of the carbide for a 0.08%C steel.

Because the diffusion distance is relatively constant with carbide size, any given thermal cycle will produce a certain characteristic diffusion distance. When this diffusion distance is more than half the distance between particles, an overlapping network of austenite will be formed, even at temperatures below the A_3 . If the steel is then cooled fast enough to transform the austenite to martensite, a brittle network will be formed. For the same thermal cycle, and consequently the same diffusion distance, large carbides are far enough apart so that only a relatively small volume around the carbides can be transformed to martensite and a continuous brittle network should be avoided.

Object

The object of this investigation was to establish, with the use of hardness data and metallographic examination, the possibility of formation of a brittle martensitic network in a 0.08%C steel.

Martensite containing C in excess of 0.20% is considered excessively brittle, whereas low C martensite generally possesses adequate toughness for engineering purposes. The only region where a high C content can be found in a low C steel is in the C gradient

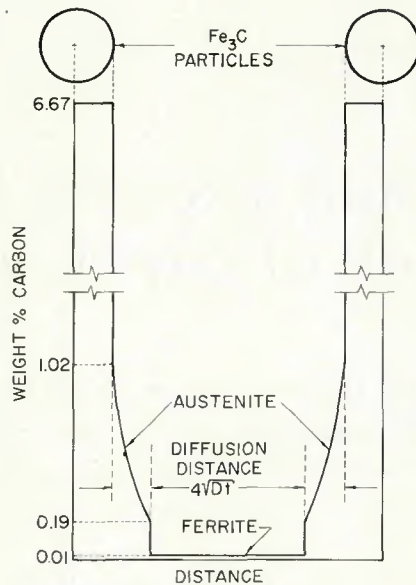


Fig. 1—Carbon concentration gradient around Fe_3C particles at 1530 F

surrounding an incompletely dissolved iron carbide particle. Therefore, this investigation also included a study of the dissolution of iron-carbide particles and the relation of the diffusion of C from these particles with temperature during the dissolution process into austenite.

Materials

The chemical composition of the two steels—0.047 in. (1.2 mm) thick—used in this investigation is as follows in wt %: steel A—0.07 C, 0.40

Mn, 0.008 P, 0.017 S; steel B—0.09 C, 0.35 Mn, 0.007 P, 0.019 S.

These steels, supplied by Rochester Products Division of General Motors, are materials typically used in the manufacture of resistance seam welded tubing. The as-received microstructures are shown in Figs. 2. Steel A differs from steel B primarily in the size of carbides. Assuming a spherical shape and a completely random distribution, the average diameter of iron carbides in steel A is 1.22 μm and in steel B, 5.30 μm .

Procedure

The thermal cycles to which the steel specimens were subjected were reproduced in a Gleeble.⁶ Rectangular specimens, each $1/2 \times 3 \times 0.047$ -in. (12.7 \times 76 \times 1.2 mm), were positioned in the Gleeble with a small jaw-separation of 0.50 in. (12.7 mm) in order to obtain a rapid cooling rate. This jaw-separation produced a controlled isothermal zone of 0.125 in. (3.2 mm) width at the center of the 3 in. (76 mm) dimension.

The Gleeble was programmed for a linear heating rate to a predetermined peak temperature, at which time the current was shut off and the specimen was allowed to cool rapidly in the water-cooled jaws. For each peak temperature investigated, triplicate samples of each of the two steels of different initial carbide size were run. In all cases, the time required to heat to peak temperature was maintained at 4 seconds (s). The exact thermal cycle was documented by using a direct-developing-type, electromagnetic oscillograph to record the output of the control thermocouple.

The specimens were sectioned in the longitudinal direction with the plane of polish parallel to the sheet thickness. After mounting, the samples were polished down to the control thermocouple bead where the exact thermal history had been recorded. Microhardness readings were taken across the thickness of the sheet, beginning at a point directly beneath the thermocouple, using a 15 gram (g) load and a Knoop indenter. The specimens were then etched and examined metallographically.

Results

The summary of microhardness readings taken on steel B (containing large carbides) is shown in Fig. 3. A load of 15 g was chosen for the microhardness test to obtain the smallest indentation possible.

At a peak temperature of 1530 F (832 C), the diffusion distance and the transformed regions were small; therefore, the hardness indentations were



Fig. 2—As-received microstructures: A (top)—steel A; B (bottom)—steel B. Nital Etch, $\times 500$ (reduced 46% on reproduction)

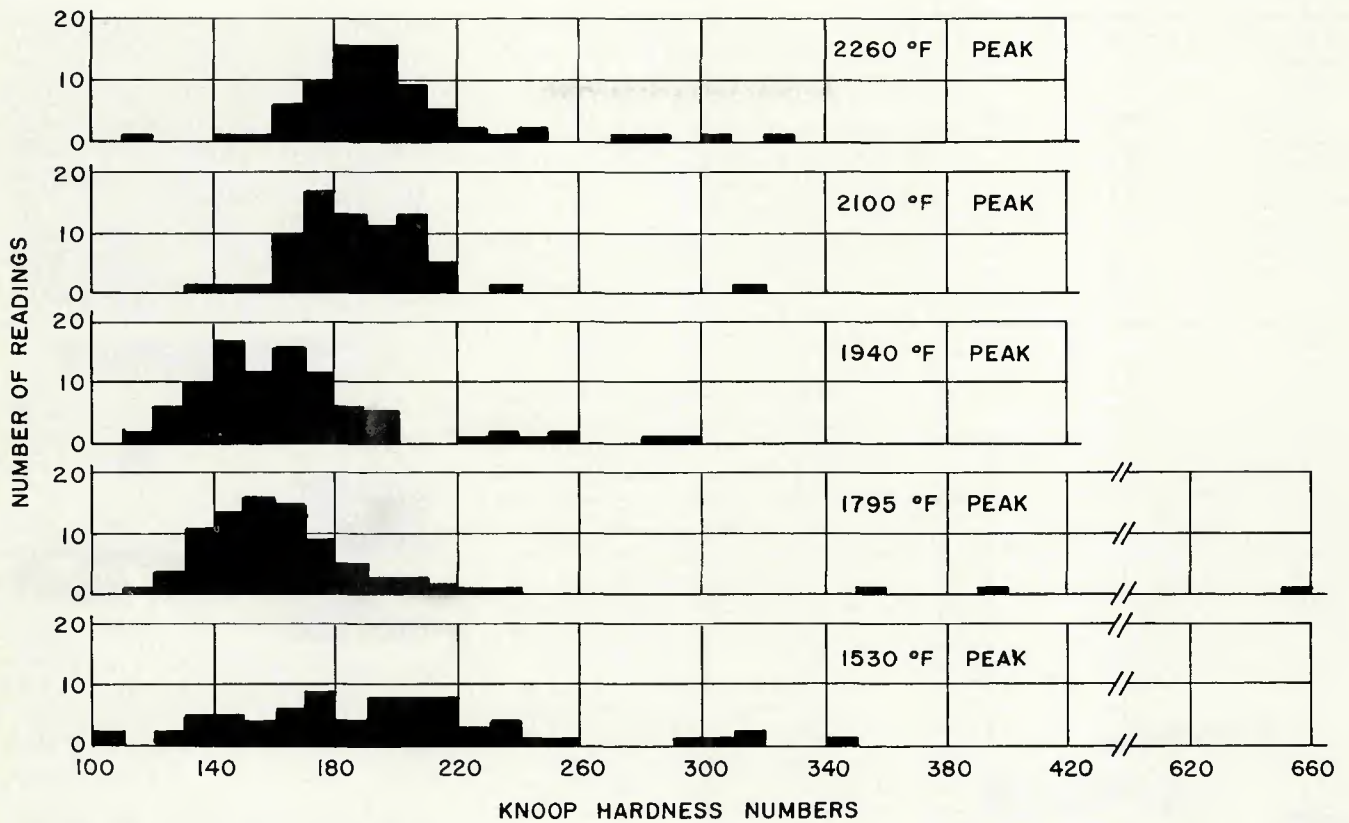


Fig. 3—Distribution of microhardness readings on steel B

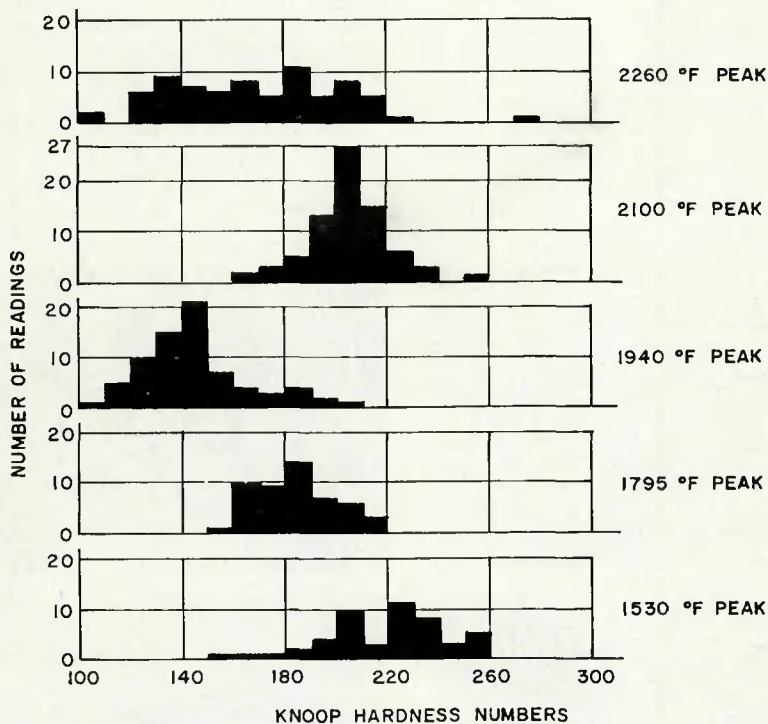


Fig. 4—Distribution of microhardness readings on steel A

large enough to represent an average of the hard and soft areas. With the specimen that experienced the 1975 F (979 C) peak temperature, the diffusion distance was large enough so that an entire indentation could be placed in the transformed region. The resulting

hardness was a Knoop reading of 655, corresponding to 62.5 on the Rockwell "C" scale. Hardness readings of 360 and 400 were also found, but in these cases the indentations were not located completely in the transformed region.

Table 1—Summary of Vickers Hardness Readings

Peak temperature		Hardness, HV ₃₀	
F	C	Steel A	Steel B
1530	832	189	178
1795	979	169	168
1940	1060	169	169
2100	1149	170	172
2260	1238	176	172

As the peak temperature increased above 1795 F (979 C), the average hardness increased, but in no case did the hardness exceed 330. This is caused by the fact that at 1940 F (1060 C) the carbides were completely dissolved and the carbon gradient was decreasing. With the width of the diffused region increasing and the maximum C% decreasing, the probability of locating an impression in a transformed region increased, but the transformed region had a lower C content and no hard areas were present.

Figure 4 shows the summary of microhardness readings on steel A which has the fine carbide dispersion. With these specimens, the hardest reading found was 280 Knoop. This low reading resulted from the fact that, even with a load of 15 g, the length of the indentation was large when compared to the transformed

Table 2—Thermal Data for Gleeble Specimens

Peak temperature, F	Heating rate, F/s	Cooling rate, F/s
1530	345	450
1795	435	535
1940	475	570
2100	505	620
2260	545	625



Fig. 5—Microstructures of steels heated to a 1530 F peak temperature: A (top)—steel A; B (bottom)—steel B. Nital etch, $\times 500$ (reduced 46% on reproduction)

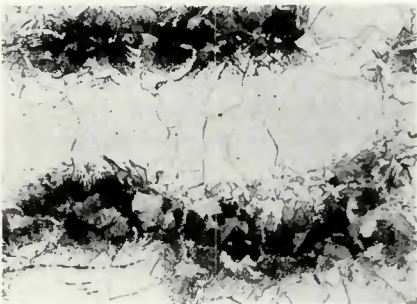


Fig. 7—Microstructures of steels heated to a 1940 F peak temperature: A (top)—steel A; B (bottom)—steel B. Nital etch, $\times 500$ (reduced 46% on reproduction)

region; consequently, the reading represented an averaged value of hardness.

It was then decided to measure the hardness using the Vickers scale and a load of 30 kg. The average Vickers hardness readings measured on duplicate samples of each of the steels following exposure to various peak temperatures are shown in Table 1. This table shows that the maximum hardness was obtained when the fine-carbide steel, steel A, was heated to a peak temperature of 1530 F (832 C).

As discussed previously, if a region of martensite should form at this low temperature, it would surround the carbide and be surrounded in turn by ferrite. The high percentage of C in the austenite formed at 1530 F (832 C) should provide a hard brittle martensite upon transformation, and this is what the hardness reading indicates. Martensitic areas should still exist in the steel with large carbides heated to a peak temperature of 1530 F (832 C). However, more ferrite is present because the intercarbide distance is large and, therefore, a somewhat lower Vickers hardness reading is found.

After the microhardness readings were taken, the specimens were etched in 2% Nital and photomicrographs were taken at a magnification of $\times 500$. The peak temperature and corresponding heating and cooling rates to which the specimens were subjected are shown in Table 2.

Figure 5 shows the microstructures of the steels A and B after exposure to a peak temperature of 1530 F (832 C).



Fig. 8—Microstructures of steels heated to a 2100 F peak temperature: A (top)—steel A; B (bottom)—steel B. Nital etch, $\times 500$ (reduced 46% on reproduction)

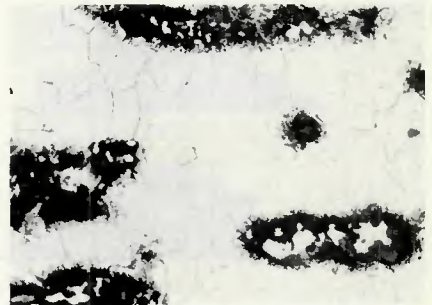
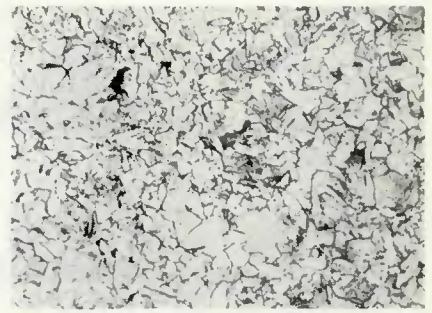


Fig. 6—Microstructures of steels heated to a 1795 F peak temperature: A (top)—steel A; B (bottom)—steel B. Nital etch, $\times 500$ (reduced 46% on reproduction)

Figure 5B clearly shows the microstructure predicted in Fig. 1. The undissolved carbides can clearly be seen in the center of the C-diffusion area. It should be noted that the specimens were etched deeply to facilitate subsequent measurements of the diffusion distances.

At a peak temperature of 1795 F (979 C), the specimens had been heated entirely into the austenite region. This is clearly evident in Fig. 6A which



Fig. 9—Microstructures of steels heated to a 2260 F peak temperature: A (top)—steel A; B (bottom)—steel B. Nital etch, $\times 500$ (reduced 46% on reproduction)

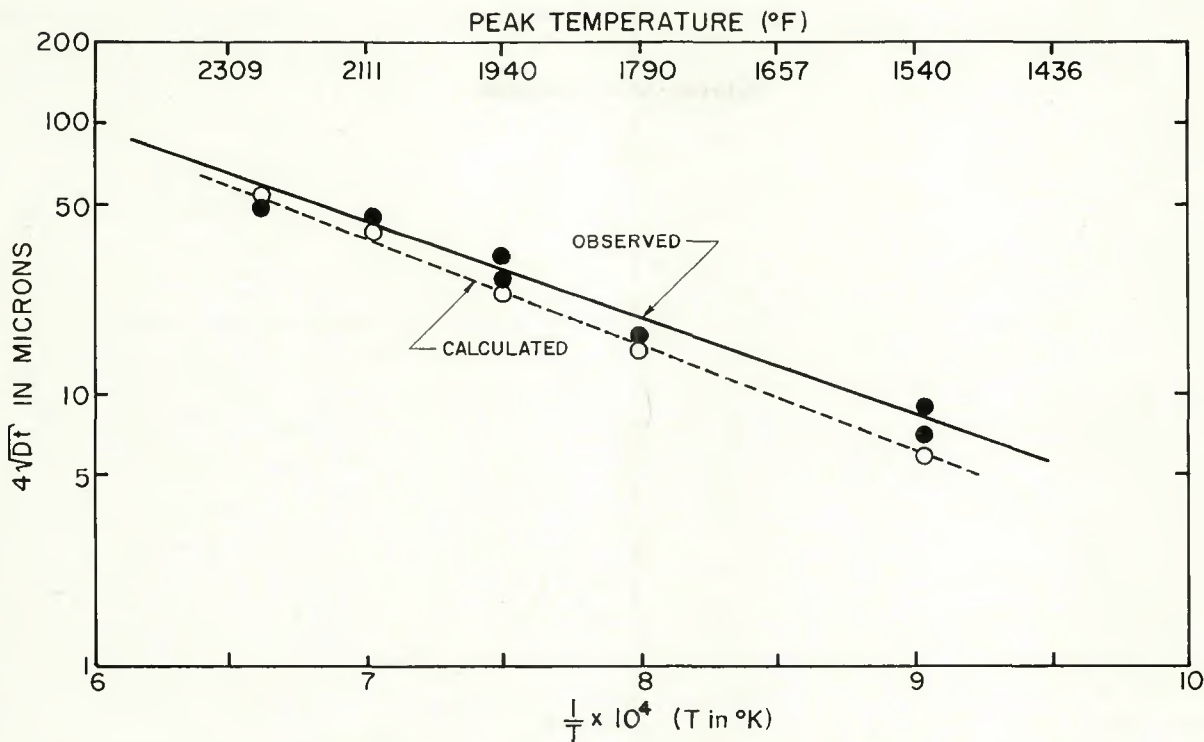


Fig. 10—Carbon diffusion distance $4(Dt)^{1/2}$ vs. reciprocal absolute temperature

shows considerable grain refinement. In Fig. 6B the C-diffused area has increased, but undissolved carbides can still be observed in the center of some of the dark-etching areas. It is also interesting to note that little grain refinement has taken place in the coarse-carbide steel.

Figure 7 shows the microstructures of the specimens that were exposed to a peak temperature of 1940 F (1060 C). As may be noted in Fig. 7A, a Widmanstätten-type structure is developing in steel A. With steel B in Fig. 7B, areas possessing a martensitic structure are evident. This was verified by sectioning a similar specimen and heating it to 400 F (204 C) for 30 min. The original light-etching areas shown in the diffused area were darkened, indicating the formation of tempered martensite.

The microstructures resulting from an exposure to a peak temperature of 2100 F (1149 C) are shown in Fig. 8. Figure 8A shows more of the Widmanstätten structure, while Fig. 8B shows that the region of C diffusion has

increased in size and contains some martensite.

The highest peak temperature investigated was 2260 F (1238 C); the resulting microstructures are shown in Fig. 9. At this temperature, both materials should be homogeneous under equilibrium conditions, but variations in C content can be seen in Fig. 9A. In Fig. 9B the C-diffusion region has increased, but the areas of high-C martensite have decreased; these microstructural changes show that the C gradient is flattening out.

With steel B, the microstructures at each peak temperature showed a C-diffusion region which could be readily measured. Therefore, a plot of the diffusion distance vs. the reciprocal of absolute temperature was prepared as shown in Fig. 10. This graph shows that the diffusion distance, $4(Dt)^{1/2}$, varies linearly with the reciprocal of the absolute temperature. The diffusion distances measured in steel B are reported in Table 3.

To see how these data compare with theoretical calculations, the method

reported in Shewmon⁷ was used for finding an effective value of time for a diffusion reaction resulting from a complex thermal cycle.

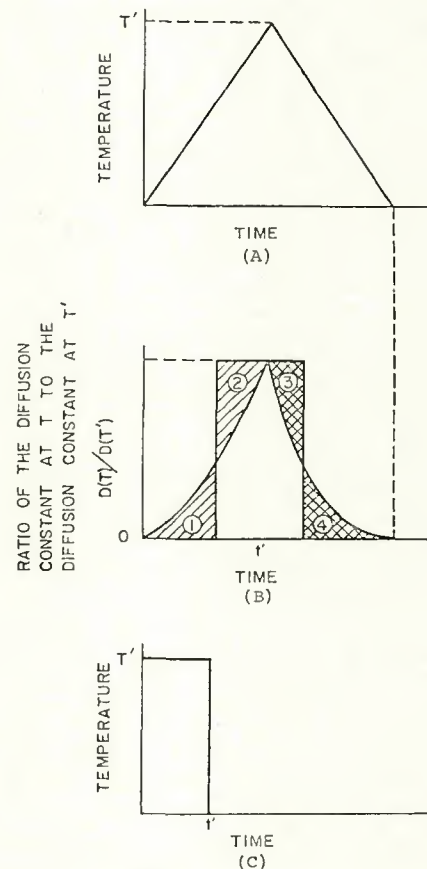


Fig. 11—Schematic of the method of determining the effective diffusion time

Table 3—Measurement of Carbon-Diffusion Distance

Peak temperature		1/T	4(Dt) ^{1/2} , μm
F	K		
1530	1105	9.05 × 10 ⁻⁴	7.3, 9.0
1795	1252	7.99 × 10 ⁻⁴	17.6
1940	1333	7.50 × 10 ⁻⁴	28.0, 34.0
2100	1422	7.03 × 10 ⁻⁴	49.0
2260	1511	6.62 × 10 ⁻⁴	50.0

Table 4—Calculation of Carbon-Diffusion Distance

Peak temperature, F	Heating time from 1340 F to peak, s	Cooling time from peak to 1340 F, s	Effective time, s	Diffusivity D, (10 ⁻⁸ cm ² /s)	Diff. dist. 4(Dt) ^{1/2} , μm
1530	0.57	0.46	0.57	4.3	6.3
1795	1.00	0.80	0.62	26.5	16.2
1940	1.24	0.99	0.73	60.4	26.6
2100	1.45	1.57	0.81	134.3	41.7
2260	1.56	1.29	0.72	271.6	55.9

The time-temperature trace from the Gleeble was marked so that zero time corresponded to the instant the specimen reached 1340 F (727 C). This was done because the carbide phase is stable until the lower critical temperature 1340 F (727 C) is exceeded. A schematic representation of the thermal cycle is shown in Fig. 11A.

The diffusivities for C in gamma iron were calculated from the equation:⁸ $D = 0.21e^{-33800/RT}$. The ratio of the diffusivity of C at a temperature below the peak, to the diffusivity of C at the peak temperature was plotted vs. time. A schematic representation of this step is shown in Fig. 11B. Next, vertical lines were constructed so that the areas labeled 1 and 2 were equal, and the areas labeled 3 and 4 were equal. The time between these vertical lines represents the effective time at peak, as is shown in Fig. 11B. Finally, Fig. 11C shows the equivalent diffusion process consisting of time, t' , at temperature, T' , which will provide the diffusion equivalent to that of the thermal cycle shown in Fig. 11A.

The average diffusion distance $4(Dt)^{1/2}$ was calculated from the equivalent times at peak temperature and the diffusion coefficients. The calculated values of $4(Dt)^{1/2}$ are shown in Table 4, and a plot of these values vs. the reciprocal of the absolute temperature is shown in Fig. 10. This plot is approximately parallel to the experimentally determined curve but is located at slightly lower values of $4(Dt)^{1/2}$. This difference has resulted from the use, in these approximate calculations, of too small a value of D. Although the D used was satisfactory for dilute solutions of C in austenite, the appropriate D would have a larger value which would be applicable for

higher C contents.

From Fig. 10, the temperature at which a continuous martensitic network may form can be found. To find the temperature, the average distance between carbides in the initial microstructure must be known. By dividing this distance by two and locating where this value of diffusion distance $4(Dt)^{1/2}$ intersects the observed curve, a value of the reciprocal of the absolute temperature is found. This temperature corresponds to the condition where the diffused areas from adjacent carbides would overlap.

The observed data in Fig. 10 can be used to find the minimum size of particles that can be permitted without the possibility of forming a martensitic network at a given peak temperature. The selected peak temperature is characteristic of the thermal cycle of a particular process. When this temperature is converted to the reciprocal of the absolute temperature, the diffusion distance can be found by referring to the observed data. In order to avoid the possibility of a martensitic network, the distance between particles must be greater than twice the diffusion distance $4(Dt)^{1/2}$ found from the experimental curve in Fig. 10.

Conclusions

1. A relationship was found between carbon-diffusion distance and the reciprocal of the absolute temperature for the thermal cycles studied in a 0.08%C steel. From this relationship, the following can be determined:

(a) The temperature at which a continuous martensitic network may form.

(b) The temperature required to cause all points in the austenite to experience some degree of carbon enrichment for a given carbide spacing.

(c) The minimum size of carbide necessary to prevent a continuous martensitic network from forming.

2. It can be concluded from this investigation that the size and distribution of the iron carbides are a major factor influencing the weldability of low-carbon steels in processes involving rapid heating and cooling, such as resistance welding.

References

1. Babcock, D. E., "Fundamental Nature of Welding—The Effects of Heating Velocities, Carbide Diffusion and Carbide Melting in Electric Spot, Flash and Resistance Welding," *Welding Journal*, 18 (8), Aug. 1939, pp. 477 to 479.
2. Stout, R. D., and Doty, W. D., *Weldability of Steels*, Welding Research Council, N.Y., N.Y. 1953, p. 86.
3. Gould, R., "A Superior Microstructure for Optimum Induction Hardening," *Metal Progress*, 80 (5), Nov. 1961, pp. 66-70.
4. Huggins, R., Udin, H., and Wulff, J., "The Formation of Austenite in Plain-Carbon Steels at High Heating Rates," *Welding Journal*, 35 (1), Jan. 1956, Research Suppl., pp. 18-s to 26-s.
5. Darken, L. S., and Gurry, R. W., *Physical Chemistry of Metals*, McGraw-Hill, N.Y., N.Y., 1953, pp. 443-445.
6. Savage, W. F., "Apparatus for Studying the Effects of Rapid Thermal Cycles and High Strain Rates on the Elevated Temperature Behavior of Materials," *Journal of Applied Polymer Science*, Vol. VI., No. 21, pp. 303-315.
7. Shewmon, P. G., *Diffusion in Solids*. McGraw-Hill, N.Y., N.Y. 1963, pp. 31-32.
8. Smithells, C. J., *Metals Reference Book*. Butterworths, London, Great Britain, 1949, p. 397.